Dalton Transactions

Accepted Manuscript

ROYAL SOCIETY OF CHEMISTRY

www.rsc.org/dalton

Dalton Transactions

RSCPublishing

ARTICLE

Syntheses, structure solutions, and catalytic performance of two novel layered silicates

Cite this: DOI: 10.1039/x0xx00000x

Jie Liang,[a] Jie Su,[*b] Yanping Chen,[a] Zhaofei Li,[c] Kuo Li,[a] Hao Zhang,[a] Xiaodong Zou,[b] Fuhui Liao,[a] Yingxia Wang,[*a] and Jianhua Lin[*a]

Received 00th February 2015,
Accepted 00th February 2015

DOI: 10.1039/x0xx00000x

www.rsc.org/

Two novel layered silicates, PKU-13 and PKU-13a, were hydrothermally synthesized by using trimethylpropylammonium hydroxide as the structure directing agent (SDA). Their structures were solved by powder X-ray diffraction data in combination with electron diffraction technique and NMR spectroscopy. These two silicates are built from the same r52 layer in different stacking modes: the adjacent r52 layers in PKU-13a take a 0.5*b* + 0.68*c* shift compared with those in PKU-13. The difference is due to the SDA cations located between the layers. The SDA cations exist as monolayer in the structure of PKU-13, and link the adjacent layers by coulomb actions in combination with strong hydrogen bonds. In PKU-13a, SDA cations present in bi-layer which expends the distance between layers and destroys the inter-layer hydrogen bonds. PKU-13a can transform to PKU-13 after the treatment by acetic acid solution. The co-existence of intra-layer hydrogen bonds in PKU-13 interfere in its condensation to ordered crystalline microporous framework. Both PKU-13 and PKU-13a exhibit good catalytic activities as base catalysts in Knoevenagel condensation reaction.

Introduction

Layered silicates are very common in nature and have been widely used as raw materials in the porcelain industry, as additives in paints and paper, as sorbents for cleaning and separation, and as catalysts in reaction processes.[1-2] Recently, the topotactic condensation of layered silicates into zeolite frameworks has received considerable attention as a synthesis strategy for the formation of new zeolites.[3-12] For example, zeolites with the framework codes **FER**, **MWW**, **CAS**, **CDO**, **NSI**, **RRO**, **RWR**, **SOD** and **MTF** could be synthesized by topotactic conversion from their hydrous layered silicate precursors PREFER[5a] (and PLS-3[5b]), MCM-22(p)[6], EU-19[7], PLS-1[8a] (and MCM-65[8b], RUB-36[8c] and PLS-4[5b]), NU-6(1)[9], RUB-39[10], R-RUB-18[11a] (and H-Oct[11b]), HAc-RUB-15[12], and HPM-2[13], respectively. Therein, **CDO**, **NSI**, **RRO**, and **RWR** have not been realized by direct hydrothermal synthesis, which indicates the great potential of this method for the formation of zeolites. From the view of the structural aspect, the top-down method[14a] and its inverse process, sigma transformation[14b], which target in designing new porous compounds by the disassembly and re-assembly of the layers in known zeolites, attracted additional attention on layered materials. These methods are not only useful for the formation of zeolites, but also helpful in understanding the build-up of zeolite structures from layered silicates.[3]

The study on the structures of layered silicates and their transformation are of interests for inducing the formation of crystalline products. A successful topotactic condensation depends on various factors, such as the inter-layer distance, the direction of opposite silanol groups in adjacent layers, and etc. Therein, the structure directing agents (SDAs) involved in the layered silicates play a significant action.[4] On one hand, different organic templates may lead to different layered silicates built by the same layer. One notable example is that the layered silicates, PLS-1[8a], PREFER[5a], and MCM-47[15], which are composed of the same fer layer but in different stacking modes, can be synthesized by employing tetramethylammonium, amino-tetramethylpiperdinium, and tetramethylene-bis(*N*-methylpyrrolidinium) in the reaction. Upon calcination, PLS-1 and PREFER transform to zeolites **CDO** and **FER** respectively, whereas MCM-47 only condenses to a highly disordered phase. On the other hand, the use of the same SDA may also induce layered silicates with different layer types. For instance, HUS-1 with ast layer[16], ERS-12 with fer layer[17], and DLM-2[18] and RUB-15[12] with sod layer are obtained by using tetramethylammonium as SDA under different synthesis conditions. Since the role of the organic cations in the formation of layered silicates is specific, the investigation of host-guest interactions between the silicate layers and the organic cations is an important subject for the formation of ordered crystalline zeolites.

Structure determination of layered silicates is challenging, especially for those which cannot fully condense to ordered structures. Firstly, layered silicates always appear in nano- or submicron-sized crystals which are too small to be studied by single crystal X-ray diffraction. Secondly, the preferred orientation related to the plate-like morphology and the severe peak broadening caused by the stacking disorder increase the difficulties of the structure determination from powder X-ray diffraction (PXRD). Thirdly, the instability of layered silicates under electron beam brings extra task in using transmission electron microscopy (TEM). Therefore, the structure determination of layered silicates is always a comprehensive process by the combination of PXRD and electron diffraction (ED) data with complimentary techniques such as solid-state NMR and thermogravimetric analysis (TGA).[19]

Here, we report the syntheses, structures and properties of two new layered silicates, PKU-13 and PKU-13a. The structures of PKU-13 and PKU-13a were revealed by employing PXRD, TEM, solid-state NMR, and elemental analysis. The procedures of the structure solutions are described in details, and the structure relations of PKU-13 and PKU-13a are presented, especially the hydrogen bonds and the distribution of organic molecules between the layers are discussed. The potential application of the two silicates as base catalysts in Knoevenagel condensation reaction was tested.

Experimental section

Synthesis of SDA

A typical procedure for the synthesis of trimethylpropylammonium hydroxide (M_3PrNOH) was described as follows. The tertiary amine, dimethylpropylamine, was first synthesized by an Eschweiler-Clarke reaction from propylamine, formic acid and formaldehyde. Then, it was reacted with methyl iodide, giving rise to trimethylpropylammonium iodide. The solid product was filtered, washed with acetone, and dried in air. The obtained quaternary ammonium iodide was characterized by ^{13}C and ^{1}H NMR spectroscopy (Fig. S1). The hydroxide form of the SDA was obtained by reaction of the trimethylpropylammonium iodide with Ag_2O in an aqueous solution. The concentration of the SDA in the solution was determined by titration with a standard HCl solution.

Synthesis of layered silicates

A certain amount of fumed silica was dispersed in the aqueous solution of M_3PrNOH, and the mixture was thoroughly stirred to form a uniform suspension. The water content was controlled by evaporation at 70 °C in an oven. The typical molar composition of the starting gel was 1 SiO_2: 0.5 SDA: 15~17 H_2O for PKU-13. PKU-13a was obtained when the SDA/SiO_2 ratio increased to 0.75. The mixture was transferred into a Teflon-lined stainless steel autoclave and heated in an oven at 155 °C with a 15 rpm rotation speed for 30 days. After quenching in cold water, the solid product was filtered and washed with distilled water, and dried at 60°C overnight. The morphologies of PKU-13 and PKU-13a are shown in Fig. S2.

The acetic acid (HAc) treatment of PKU-13a was performed as follows. Typically, 0.02 g of PKU-13a was immerged into 5 mL HAc solutions with different concentrations (0.6, 2, 6, 10, and 17 $mol \cdot L^{-1}$) and stirred overnight. The mixture was then transferred into a Teflon-lined stainless autoclave and heated at 100 °C for 3 days. After cooling down, the solid product was filtered, washed with distilled water and dried at 60°C overnight.

Characterizations

Powder X-ray diffraction (PXRD) pattern of PKU-13 was recorded on a Bruker D8 Advance diffractometer in modified Debye-Scherrer geometry, using a Cu $K\alpha_1$ radiation source (λ = 1.5406 Å) with a germanium monochromator and a PSD detector. PXRD pattern of PKU-13a was collected on a PANalytical X'Pert PRO MPD diffractometer in transmission geometry using Cu Kα radiation (λ = 1.5418 Å), and the sample was packed into a 0.5 mm borosilicate capillary. *In-situ* PXRD data were collected from 50 to 400 °C with an increment of 50 °C per step on a Bruker D8 Advance diffractometer. The temperature was kept for 2 minutes at each stage before the data collection. Samples for TEM observations were crushed, dispersed in absolute ethanol and treated by ultra-sonication for 5 min. A droplet of the suspension was transferred onto a carbon-coated copper grid. Three-dimensional (3D) rotation electron diffraction (RED) data of PKU-13 and PKU-13a samples were collected under 200 kV using the software RED – data collection[20] on a JEOL JEM2100 TEM. A single-tilt tomography sample holder was used for the data collection, which could tilt from -70° to +70° in the TEM. The morphology and crystal size of PKU-13 and PKU-13a were evaluated using a Quanta 200F scanning electron microscope (SEM). Elemental analysis for carbon, nitrogen and hydrogen was carried out with an Elementar Vario EL III microanalyzer. Thermal analysis of the as-synthesized samples was performed on a TGA Q50 V20.6 thermal analyzer with a heating rate of 10 °C/min from 25 to 800 °C in air. Solid-state ^{29}Si MAS and ^{13}C CP MAS NMR spectroscopy were performed on a Bruker ASX 400 NMR using 5 mm Bruker probes. For quantitative signal intensities in the ^{29}Si experiments, high power decoupling was used with a 45° impulse length of 1.9 μs and delay time between pulses of 120 s. Solid-state ^{1}H-^{29}Si CP MAS NMR spectra were measured with a contact time of 3 ms. The ^{13}C CP MAS NMR spectra was measured with a spinning frequency of 10 kHz and a cycle delay time of 2 s.

Structural analysis

The Rietveld refinements of PKU-13 and PKU-13a by PXRD data were performed using Topas Academic V4.1.[21] Background was fitted with a Chebychev polynomial function (13^{th} order for PKU-13, 15^{th} order for PKU-13a). Pearson VII function was used to fit the peak shape. Soft restraints were placed on the Si-O bond lengths (1.62 Å) and the O…O distances (2.64 Å) between oxygen atoms in one tetrahedron

during the refinement. The M_3PrN^+ cation without the hydrogen atoms was introduced as a rigid body and located by simulated annealing algorithm. Atoms with the same elemental type were constrained to have the same isotropic thermal displacement parameters.

Catalytic tests

Using PKU-13 and PKU-13a as the catalysts, the Knoevenagel reactions were carried out as follows. A mixture of benzaldehyde (1.0 mmol), ethyl cyanoacetate (1.2 mmol), and naphthalene (0.1 mmol, as an internal standard) in methanol (0.5 ml) was added to a flask containing the layered silicates (~25 mg). After stirring for 2-7 hours at 25-70 °C, the resulting mixture was filtrated to remove the catalyst. The filtrate was analyzed by gas chromatograph to identify the products and detect the conversion of benzaldehyde.

Results and discussions

Synthesis

The synthesis conditions of PKU-13 and PKU-13a are summarized in Table S1 in Electronic Supporting Information (ESI). It can be seen that the water content and the ratio of SDA over silica are the key factors for the formation of PKU-13 and PKU-13a. When the H_2O/SiO_2 ratio was kept in the range of 15-17, crystalline PKU-13 could be realized with the M_3PrNOH/SiO_2 molar ratio of 0.5. The decrease of the M_3PrNOH/SiO_2 ratio to 0.35 yielded a NON type zeolite, while the increase of the M_3PrNOH/SiO_2 ratio to 0.75 led to PKU-13a. The decrease of water content yielded an amorphous material, while an increase of water content led to a **NON** type zeolite. The main difference between the synthesis conditions of PKU-13 and PKU-13a is the amount of SDA, with the SDA/SiO_2 ratio of 0.5 for PKU-13 and 0.75 for PKU-13a.

Solid state NMR study

In the solid state ^{13}C spectra of PKU-13 and PKU-13a (Fig.S3 in ESI), four main peaks corresponding to C atoms in the propyl and methyl groups are observed. From an overview, the ^{13}C NMR spectra of PKU-13 and PKU-13a are similar to the responses of C atoms in *n*-propyltrimethylammonium iodide (Figure S1b), which demonstrate that the SDAs are intact in the two compounds. As the differences of the C-13 MAS NMR spectra of PKU-13 and PKU-13a at around 65-70 ppm that relates to the C atom (C1) directly linking to N atom in propyl group, it reflects the different distribution of the SDA cations in the two compounds. The narrow lines of PKU-13 (Fig. S3a) imply that the SDA is located in a distinct way, either quite mobile in a unique position in pore space, while the broader lines of PKU-13a (Fig S3b) are due to slight positional disorders. The situation is even worse for C4 in PKU-13a (~ 10ppm) which has the highest degree of freedom and might be located in different geometric orientations leading to the signal splitting. Since NMR is very sensitive to geometric distortions and local environment whereas XRD averages structural features over time and space, these feature become visible in the NMR, the structure analysis by PXRD, however, cannot reveal these subtle details.

The ^{29}Si MAS NMR spectra of PKU-13 and PKU-13a are similar, as shown in Fig. 1, which indicates that the chemical environments of silicon are similar in these compounds. In the spectrum of PKU-13 (Fig. 1a), the three peaks centered at -98, -99, -101 ppm can be assigned to Q^3 units [$(-SiO)_3Si-OH$ and $(-SiO)_3Si-O^-$], and the peaks at -106, -109, -116 ppm are assigned to Q^4 units [$(-SiO)_4Si$]. The peak assignment is evidenced by the ^1H-^{29}Si CP NMR spectrum (Fig. S4a), in which the relative intensities of the three peaks at -98, -99, -101 ppm are enhanced, indicating that they are associated with hydroxyls. In the spectrum of PKU-13a (Fig. 1b), the two signals located at -97 and -100 ppm belong to Q^3 units, and the remaining three signals at -105, -109 and -116 ppm belong to Q^4 units. The estimated ratio of Q^4/Q^3 peak intensity is about 1.5 for both of PKU-13 and PKU-13a, which indicates the existence of a large number of silanol groups in the structures. The ^{29}Si MAS NMR and ^1H-^{29}Si CP NMR results indicate that PKU-13 may take a layered structure.

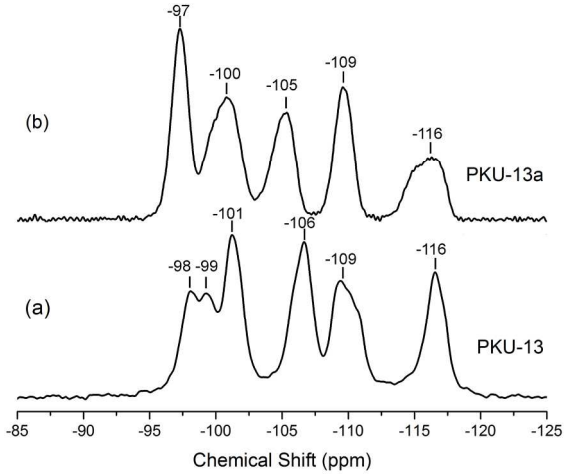

Fig. 1 Solid state ^{29}Si MAS NMR spectra of (a) PKU-13 and (b) PKU-13a.

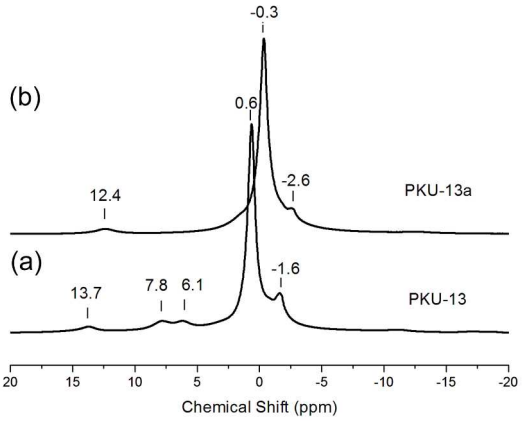

Fig. 2 Solid state ^1H MAS NMR spectra of (a) PKU-13 and (b) PKU-13a.

The ^{1}H MAS NMR spectra of PKU-13 and PKU-13a are represented in Fig. 2. The chemical shifts of protons from the M_3PrN^+ cations are observed at 0.6 and -1.6 ppm for PKU-13 and -0.3 and -2.6 ppm for PKU-13a. In the ^{1}H NMR spectrum of PKU-13 (Fig. 2a), the three signals at 6.1, 7.8 and 13.7 ppm are the responses of hydrogen atoms in silanol groups, which are involved in strong hydrogen bonding. Corresponding O…O distances are calculated to be 2.77, 2.71 and 2.53 Å, according to the equation δ/ppm=90.3-30.4×d(O…O)/Å.[22] In the ^{1}H NMR spectrum of PKU-13a, there is only one peak at 12.4 ppm related to hydrogen bonding, which corresponds to a d(O…O) of 2.56 Å (Fig. 2b). Similar chemical shift values caused by H-bonds of silanol groups have been observed in many layered silicates, such as RUB-18 (15.9 ppm)[23], MCM-47 (16.6 ppm)[5], RUB-39 (16.4 ppm)[10], and HUS-2 (6.7 and 13.5 ppm)[24b]. The different ^{1}H NMR spectra of PKU-13 and PKU-13a implies the presence of different H-bonds between neighbouring siloxy/silanol groups.

Structure determination of PKU-13

The PXRD pattern of PKU-13 was primarily indexed by a triclinic cell with the lattice parameters a = 10.61 Å, b = 7.49 Å, c = 9.26 Å, α = 112.7°, β = 85.4° and γ = 107.2° using the program McMaille.[25] Rotation electron diffraction (RED)[20], a newly developed method for collecting 3D electron diffraction data, was used to re-exam the lattice parameters. The 3D reciprocal lattice of PKU-13 was reconstructed as shown in Fig. 3. The unit cell parameters determined from the RED data are a = 10.51 Å, b = 7.439 Å, c = 9.241 Å, α = 111.27°, β = 86.15° and γ = 106.85°, which are consistent with those obtained from PXRD. The possible space groups are $P1$ and P-1. Since most zeolite-related materials are centrosymmetric, we first selected the centrosymmetric space group P-1 for PKU-13. Combining the TGA (Fig. S5a) and CHN analysis (Table S2) results, the chemical formula of PKU-13 is estimated to be $[Si_{10}O_{19}(OH)_3](C_6H_{17}N)$.

By literature searching, we noticed that the unit cell parameters PKU-13 are similar to those of two layered silicates, RUB-52[24a] (P-1, a=9.267 Å, b=12.499 Å, c=7.404 Å, α=98.09°, β=112.21°, γ=69.54°), and HUS-2[24b] ($P2_1/c$, a=7.3434 Å, b=23.582 Å, c=9.5843 Å, and β=116.0°). They show almost the same unit areas, i.e. 64.0 Å^2 of $bc\sin\alpha$ for PKU-13, 63.6 Å^2 of $ac\sin\beta$ for RUB-52 and 63.3 Å^2 of $ac\sin\beta$ for HUS-2, which indicates that PKU-13 may possess the same r52 layer as the two known silicates. Considering the adjacent layers in HUS-2 are related by mirror symmetry, and the length of repeat unit perpendicular to the layers in HUS-2 is almost twice as that in PKU-13, we assume that the adjacent layers in PKU-13 have the common orientation, like those in RUB-52. If the stacking sequence in HUS-2 is defined as …$ABAB$…along the b direction, the stacking sequence in PKU-13 is …$AAAA$… along the a direction, similar to that in RUB-52 along the b direction. Recently, HUS-7[24c] ($C2/c$, a=17.111 Å, b=7.3945 Å, c=33.025 Å, and β=94.4°), a new layered silicate formed by the r52 layer was also reported. This indicates that the formation of new r52 layer in hydrothermal conditions is common, which may provide more evidences for the study of the mechanism of the formation of zeolites.

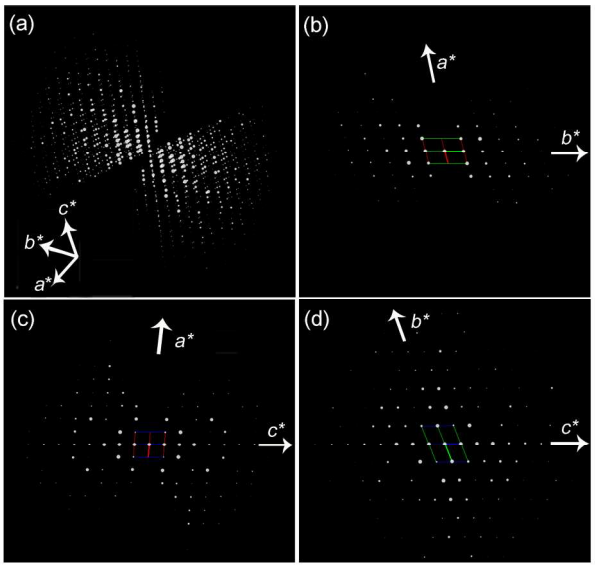

Fig. 3 (a) The 3D reciprocal lattice of PKU-13 reconstructed from the RED data, (b-d) 2D slices cut from the reconstructed 3D reciprocal lattice showing the (b) ($h0l$), (c) ($hk0$) and (d) ($0kl$) plane.

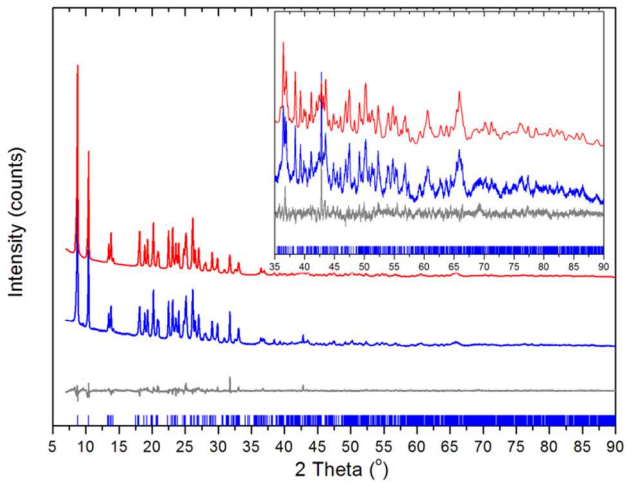

Fig. 4 Rietveld refinement of dehydrated PKU-13. The curves from the top to the bottom are simulated (red), observed (blue), and difference profiles (black), respectively; the bars below the curves indicate peak positions.

An initial model for PKU-13 was built and further refined on the basis of the PXRD data. Five independent Si and eleven O atoms were located in the asymmetric unit. Since the CHN analysis (Table S2) and solid-state ^{13}C NMR spectrum (Fig. S3) of PKU-13 indicated that the organic M_3PrN^+ cation was intact in the final product, the molecular structure of M_3PrN^+ cation (without H atoms) was introduced as a rigid body in the structure analysis. The Rietveld refinement of the final structure model converged to an R_{wp} value of 6.34%. The crystal data and structure refinement details are given in Table 1. The Rietveld refinement plots are presented in Fig. 4. The atomic coordinates, and selected bond distances and angles of PKU-13 are listed in Tables S3 and S4 in ESI.

Table 1 Powder X-ray data collection conditions, crystallographic data, and results of Rietveld analysis of PKU-13 and PKU-13a.

Compound	PKU-13	PKU-13a
Formula	$(C_6H_{17}N)_{0.5}[Si_5O_{9.5}(OH)_{1.5}]$	$(C_6H_{17}N)[Si_5O_{10}(OH)]$
Formula weight	378.57	429.67
Temperature (K)	293	293
Wavelength (Å)	1.5406	1.5418
Crystal system	triclinic	triclinic
Space group	*P*-1 (No. 2)	*P*-1 (No. 2)
a (Å)	10.6156(12)	12.6249(15)
b (Å)	7.4837(8)	7.3962(4)
c (Å)	9.2501(9)	9.2524(6)
α (°)	112.663(4)	112.006(6)
β (°)	85.367(3)	72.250(7)
γ (°)	107.158(3)	88.529(6)
Volume (Å^3)	646.49	753.24
Z	2	2
2 θ range	5°< 2θ <90°	4°< 2θ <85°
No. of parameters	108	115
No. of data points	4204	4788
R_p /R_{wp} /R_{exp}	0.0634/0.0477/0.0273	0.0715/0.0555/0.0339
R_{bragg}	0.0301	0.0225
GOF	2.32	2.18

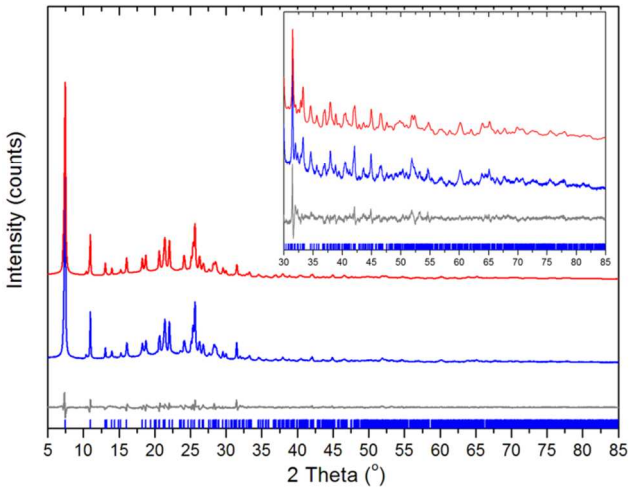

Fig. 6 Rietveld refinement of dehydrated PKU-13a. The curves from the top to the bottom are simulated (red), observed (blue), and difference profiles (black), respectively; the bars below the curves indicate peak positions.

Structure determination of PKU-13a

Structure solution of PKU-13a is similar to that for PKU-13. The triclinic unit cell parameters, a = 12.56 Å, b = 7.369 Å, c = 9.117 Å, α = 112.83°, β = 72.66°, and γ = 86.10°, were determined from the reconstructed 3D reciprocal space using RED data (Fig. 5). The similar lattice parameters b, c and the angle α of PKU-13a to those of PKU-13 indicated that PKU-13a may have the same silicate layer as that in PKU-13. The space group of PKU-13a was also assigned as *P*-1 as for PKU-13. From thermogravimetric (Fig. S5b) and CHN analyses (Table S2), the chemical formula of PKU-13a is assumed to be $(C_6H_{17}N)[Si_5O_{10}(OH)]$.

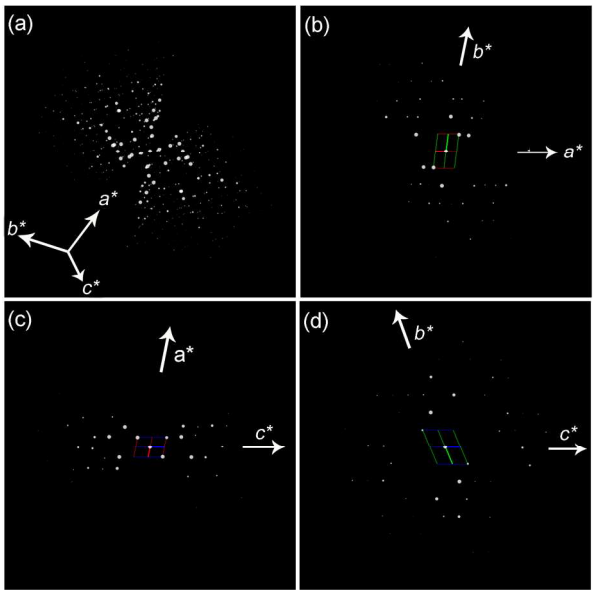

Fig. 5 (a) The 3D reciprocal lattice of PKU-13a reconstructed from the RED data, (b-d) 2D slices cut from the reconstructed 3D reciprocal lattice showing the (b) (*h*0*l*), (c) (*hk*0) and (d) (0*kl*) plane.

The starting model of PKU-13a for the Rietveld refinement against the PXRD data was built based on the framework of PKU-13. Five independent Si and eleven independent O sites are found in the asymmetric unit cell. This is consistent with the observation of the five resonance peaks in the ^{29}Si MAS NMR spectrum (Fig. 1b). The organic M_3PrN^+ (without H atoms) cation was introduced as a rigid body in the refinement. The final Rietveld refinement converged to an R_{wp} value of 7.14% as summarized in Table 1. The Rietveld refinement plot is shown in Fig. 6. The atomic coordinates, and selected interatomic distances and bond angles are listed in Tables S5 and S6 in ESI.

Crystal structure of PKU-13 and PKU-13a

The framework of PKU-13 and PKU-13a are closely related: both of them are composed of the r52 layer which is made of *bre* cage by ten silicon atoms (Fig. 7a)[24]. Within the layer, one *bre* cage connects with four neighbouring cages, resulting in the formation of six Q^4-type (Si1×2, Si2×2, Si4×2) and four Q^3-type Si atoms (Si3×2, Si5×2). The Q^4/Q^3 ratio of 3/2 is consistent with the estimated value of 1.5 from the ^{29}Si NMR spectra. Concerning the oxygen atoms, four terminal oxygen atoms (two O5 and two O10) are located in each layer. It is noticeable that a strong H-bond with an O5…O10 distance of about 2.5 Å is found within the silicate layer, giving rise to the signals at 13.4 and 12.5 ppm in the ^{1}H NMR spectra of PKU-13 and PKU-13a, respectively. Such a strong intra-layer hydrogen bond was also observed in other layered silicates, such as HUS-1[16], β-Helix-Layered-Silicate[26] and RUB-55[27] (with ast layer), RUB-18 (with rwr layer)[23], and RUB-15[28] and RUB-51[39] (with sod layer). The intra-layer hydrogen bonding has significant influence on the condensation process of layered silicates and will be discussed later.

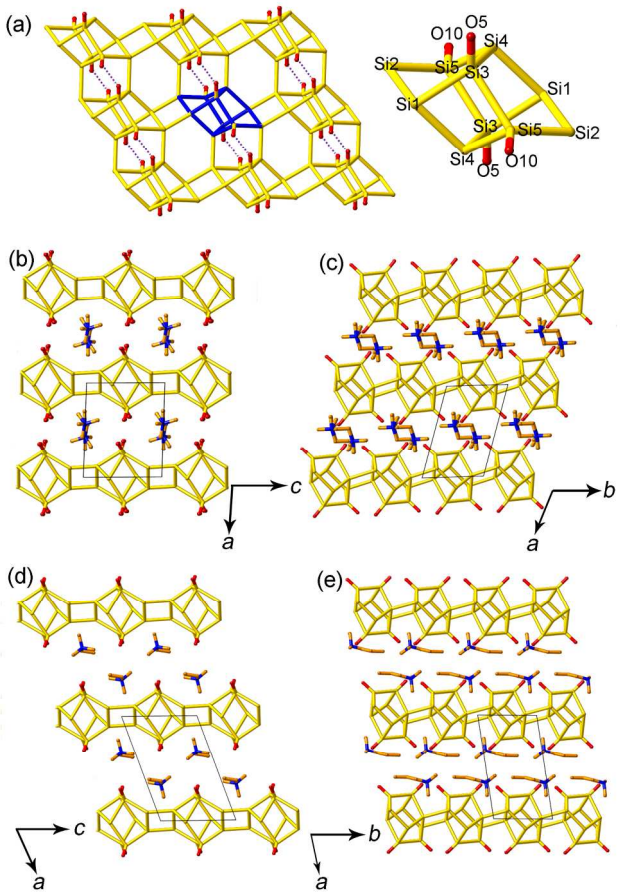

Fig. 7 Structures of PKU-13 and PKU-13a. (a) r52 layer and *bre* cage. The projection of PKU-13 along the (b) [010] and (c) [001] directions. The projection of PKU-13a along the (d) [010] and (e) [001] directions. For clarity, only the terminal oxygen atoms are shown in red. The Si-Si connections are shown in yellow, the carbon atoms in the SDA in orange, and the nitrogen atoms in blue. One of the *bre* cage is highlighted by dark blue in (a). The intra-layer hydrogen bonds are marked as the purple dotted lines in (a).

Fig. 7b and 7c show the projections of PKU-13 along the [010] and [001] directions. The layers in PKU-13 have the same orientation in the *bc*-plane. As it is aforementioned, the inter-layer distance between terminal oxygen atoms are one of the key factors in the successful topotactic condensation of layered silicates. In PKU-13 framework, we found between the adjacent layers, the distance of terminal O5 atom to O10 atom is ~2.4 Å, which is close to the intra-layer O5…O10 distance of ~2.5 Å. Thus, both intra-layer hydrogen bonds of O5…H…O10, and inter-layer hydrogen bonds O5…H…O5 exist in PKU-13 framework. It is noted that O5 atoms participate in both hydrogen bonds; half of them are protonated while the remaining O5 atoms acting as H-acceptor. This may explain the peak splitting (6.2 and 7.8 ppm) in the ^{1}H NMR spectrum. Besides, since the Si3 atoms are directly bonded to O5 atoms, the different interactions between Si3 and O5 atoms may also cause the peak splitting (-98 and -99 ppm) in the ^{29}Si NMR spectrum.

In the inter-layer region, M_3PrN^+ cations with occupancy of 0.5 are encapsulated within the pseudo 8-ring micropores. The positively charged trimethylammonium group on the SDA points toward the anionic silicate layer, while the propyl group toward the interspace of the layers (Fig. 7b). The strong H-bonds between the terminal O5…O5 atoms, and the coulomb interaction of the SDA cations M_3PrN^+ with the silicate layers attract the layers to form the 3D structure (Fig. 7b).

The projections of PKU-13a along the [010] and [001] directions are shown in Fig. 7d and 7e. Similar to PKU-13, the adjacent layers in PKU-13a have the same orientation in the *bc*-plane. Compared with those in PKU-13, the layers in PKU-13a are alternately shifted by 0.5*b* and 0.68*c* along the [010] and [001] directions, respectively. The distance between inter-layer silanol groups is 3.6 Å in PKU-13a, much larger than that in PKU-13 (2.4 Å), and there is no inter-layer H-bonds between the adjacent layers in PKU-13a. In the inter-layer region, one fully occupied M_3PrN^+ cation is observed which is different from the half occupied M_3PrN^+ cation in PKU-13. Because the positive centers of the SDA molecules are positioned near the negative centers of the silicate layers, and the propyl groups on the SDAs are found extending along the *b*-axis, the M_3PrN^+ cations in PKU-13a are oriented parallel to the layers in double layers to separate the r52 layers. The different SDA orientations (perpendicular or parallel to the layer), plus the interactions between SDA and the silicate layers may explain the different layer stacking arrangement in PKU-13 and PKU-13a.

A further comparison of PKU-13 and PKU-13a with HUS-2 and HUS-7 is interesting. These four layered silicates are built from the same r52 layer with different layer arrangements, as shown in Fig. S6. In PKU-13 and PKU-13a, adjacent layers are related by centre of symmetry, whereas in HUS-2 these layers are related by mirror planes. The relation of adjacent layers in HUS-7 is more complex: neighboring layers have a rotation of 45° around *b*-axis, and related each other by mirror plane. There is no inter-layer hydrogen bonds in PKU-13a, HUS-2 and HUS-7 due to the far distance between adjacent layers, while inter-layer hydrogen bonds exists in PKU-13. An exploration of the roles of the organic cations in the formation of the four layered silicates (propyltrimethylammonium for PKU-13, and PKU-13a, choline for HUS-2, and benzyltrimethylammonium for HUS-7) shows that their interactions with the r52 layers are similar, that is, the positive trimethylammonium groups of these SDAs point toward the negative centers of the silicate layer, inducing the formation of the layer (Fig. S7). Meanwhile the left organic groups point toward the interlayer space, resulting in the different stacking sequences of the r52 layers, as shown in Fig. S6. Thus, it seems that the ionic interaction between the SDA and terminal Si-O- groups plays an important role in the formation of r52 layers, while the distribution of the SDA cations affect the arrangement of the r52 layers.

Calcination of PKU-13 and transformation of PKU-13a to PKU-13

Since the inter-layer distance in PKU-13a is much larger than PKU-13, it is anticipated that PKU-13a cannot condense to 3D zeolites by direct heating treatment. For PKU-13, the inter-layer distance of *d*(O…O)=2.4 Å meets the demands for the

topotactic condensation, though the attempts of the calcinations of PKU-13 did not lead to ordered frameworks. The *in-situ* temperature variable PXRD pattern is shown in Fig. S8. With increasing the temperature from 50 °C to 400 °C, the crystallinity of PKU-13 decreases along with the appearance of a disordered material. The failure of the topotactic condensation of PKU-13 may be due to the close O10…O5 distance (2.5 Å) within the layers, which causes a competitive condensation between the inter-layer and intra-layer –OH groups during calcination.[4] As already mentioned , several layered silicates also suffer from the intra-layer condensation. To relieve this side effect, further chemical modifications, such as ion exchange, silylation or acid treatment were applied and succeed in some cases for the formation of zeolites.[3,11,12,30].

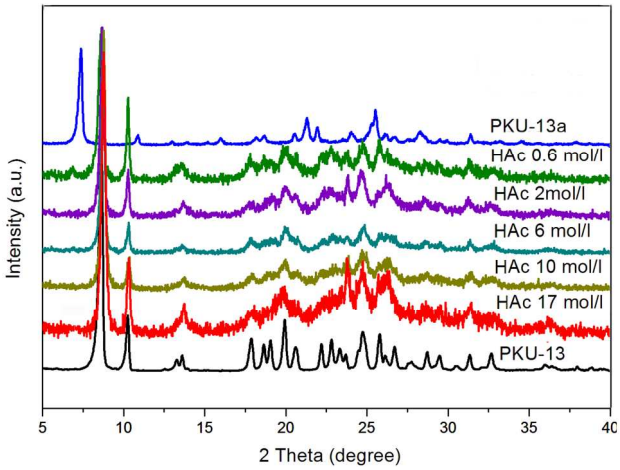

Fig. 8 PXRD patterns of PKU-13a before and after being treated with HAc at different concentrations. The bottom one is from pure PKU-13 samples.

PKU-13 and PKU-13a were treated by TEOS and acetic acid respectively. There is no significant change in the PXRD patterns for PKU-13. However, it was surprising that the treatment of PKU-13a by acetic acid caused its transformation to PKU-13, as shown by the PXRD patterns in Fig. 8. The CHN analysis in Table S2 shows that the content of organic templates in the acid-treated product is decreased, which means that some organic cations are driven out from the structure during the treatment, which may explain the phase transformation of PKU-13a to PKU-13. Since the layer in PKU-13 is unprecedented in silicate zeolites, it is worthy to make further efforts to modify PKU-13 to induce the ordered conversion.The successful condensation of PKU-13 may result in a new zeolite framework with a one-dimensional 10-ring channel system, as shown in Fig. S9. Since the r52 silicate layers in PKU-13 are distributed properly with the opposite hydroxyl groups towards one another, it may take a direct condensation to form a 3D framework with no need to shift the layer. Then, the hypothetical zeolite framework is created by connecting the related silicon atoms from the neighbouring layers.

Knoevenagel condensation reaction over PKU-13 and PKU-13a

Knoevenagel condensation is a classic C-C bond formation reaction in organic chemistry.[31]These condensations between aldehydes or ketones and active methylene compounds are often catalysed by amines or alkaline alkoxides in organic solvents.[32] Recently, layered silicates were applied as catalysts and showed notewothy activities in the Knoevenagel condensation.[24b,33] PKU-13 and PKU-13a were tested as heterogeneous catalysts for the the reaction of benzaldehyde with ethyl cyanoacetate. The reaction results under different conditions are summarized in Table 2. It was observed that the catalytic activity of PKU-13 increased with the increase of reaction temperature. When the reaction was conducted at 70°C for 7 hour, the product yield can be reached up to 97.7%. For PKU-13a, the product yield reached 94.4% at 70°C in only 3.5 hour. The catalytic activity of PKU-13a is similar to that of the layered silicate HUS-2 and PLS-1, and both are better than that of PKU-13. The better kinetics of PKU-13a than that of PKU-13 is probably due to the larger SDA amounts in the inter-layer region.

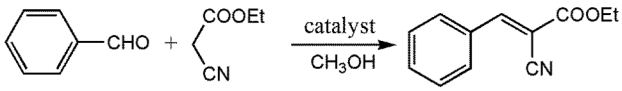

Scheme 1 Conversion of benzaldehyde to ethyl-2-cyano-3-phenylacrylate, by using PKU-13 or PKU-13a as the solid catalyst.

Table 2 Knoevenagel condensation reaction over PKU-13 and PKU-13a.

No.	Catalyst	Temperature (°C)	Time (hours)	Yield (%)
1	PKU-13	25	3.5	14.6
2	PKU-13	40	3.5	52.3
3	PKU-13	70	2	31.7
4	PKU-13	70	3.5	79.1
5	PKU-13	70	5	94
6	PKU-13	70	7	97.7,92.7[a],88[b]
7	PKU-13a	70	3.5	94.4

a 2nd use and *b* 3rd use.

Recycle experiments using PKU-13 as the catalyst were conducted at 70°C for 7 hours. The conversion of the reactants decreases slightly to 92.7% and 88.0% for the second and third cycle respectively. PXRD analysis evidences that the framework of PKU-13 is retained after the third recycle (Fig. S10). Elemental analyses of C, H and N of the samples after the catalytic cycles showed no significant difference, indicating no extraction of M_3PrN^+ cations in the inter-layers (Table S2). These results suggest that PKU-13 and PKU-13a exhibit good catalytic activity in Knoevenagel reaction, and they, together with other layered silicates can be considered as practical alternatives for soluble base catalysts in the reaction.

Conclusions

Using a simple M_3PrNOH as the SDA, two new layered silicates, PKU-13 and PKU-13a, were hydrothermally synthesized. These two compounds contain the same silicate layer r52, but with different stacking modes along the *a*-axis.

The adjacent layers in PKU-13a have a 0.50*b* + 0.68*c* shift as compared with those in PKU-13. The different orientations of M_3PrN^+ cations located in the inter-layer region play an important role in the layer stacking in PKU-13 and PKU-13a. The competition between intra-layer and inter-layer hydrogen bonding in PKU-13 hinders the successful topotactic condensation by direct heating. After the acetic acid treatment, PKU-13a can transform to PKU-13. Both layered silicates show potential as base catalysts in Knoevenagel condensation reaction.

Acknowledgements

This work was financially supported by the State Science and Technology Commission of China (2012CB224802) and the National Natural Science Foundation of China (21171009, 11275012). The TEM work is supported by the Swedish Research Council (VR), the Swedish Governmental Agency for Innovation Systems (VINNOVA), and the Knut & Alice Wallenberg Foundation through a grant for purchasing the TEM and the project grant 3DEM-NATUR. Jie Su was supported by a post-doctoral grant from the Wenner-Gren Foundation.

Notes and references

[a]College of Chemistry and Molecular Engineering, Peking University, Beijing 100871, China.
[b]Berzelii Centre EXSELENT on Porous Materials and Inorganic and Structural Chemistry, Department of Materials and Environmental Chemistry, Stockholm University, Stockholm 106 91, Sweden
[c]Petrochemical Research Institute of Petrochina, Beijing 100195, China
Electronic Supplementary Information (ESI) available: SEM images, solid-state 13C MAS NMR spectra, liquid-state 13C MAS NMR spectra, TG curves, in situ PXRD patterns, the CHN analysis, the synthetic conditions, and the atomic coordinates, and representative bond distances and angles of PKU-13 and PKU-13a are listed in supporting information. See DOI: 10.1039/b000000x/

1 E. R. Cooper, C. D. Andrews, P. S. Wheatley, P. B. Webb, P. Wormald and R. E. Morris, *Nature*, 2004, **430**, 1012.
2 (a)W. Xu, J. Dong, J. Li, J. Li and F. Wu, *J. Chem. Soc., Chem. Commun.*, 1990, **10**, 755; (b)M. Matsukata, M. Ogura, T. Osaki, P. R. H. P. Rao, M. Nomura and E. Kikuchi, *Top. Catal.*, 1999, **9**, 77. (c) A.Corma, V. Fornes, J. Martinez-Triguero and S. B. Pergher, *J. Catal.*, 1999, **186**, 57; (d) I. Rodriguez, M. J.Climent, S.Iborra, V. Fornes, A. Corma *J. Catal.*, 2000, **192**, 44; (e) T. De Baerdemaeker, H. Gies, B. Yilmaz, U. Müller, M. Feyen, F. Xiao, W. Zhang, T. Yokoi, X. Bao and D. E. De Vos, *J. Mater. Chem. A*, 2014, **2**, 9709.
3 (a) W. J. Roth, P. Nachtigall, R. E. Morris and J. Čejka, *Chem. Rev.*, 2014, **114**, 4807; (b) W. J. Roth and J. Čejka, *Catal. Sci. Technol.*, 2011, **1**, 43; (c) N. Takahashia and K. Kuroda, *J. Mater. Chem.*, 2011, **21**, 14336; (d) Z. Wang, J. Yu and R. Xu, *Chem. Soc. Rev.*, 2012, **41**, 1729; (e) F. S. O. Ramos, M. K. de Pietre and H. O. Pastore, *RSC Adv.*, 2013, **3**, 2084. (f) H. Gies, U. Müller, B. Yilmaz, T. Tatsumi, B. Xie, F. Xiao, X. Bao, W. Zhang, and D. De Vos, *Chem. Mater.* 2011, **23**, 2545.
4 B. Marler and H. Gies, *Eur. J. Mineral*, 2012, **24**, 405.
5 (a)L. Schreyeck, P. Caullet, J. C. Mougenel, J. L. Guth and B. Marler, *Microporous Mater.*, 1996, **6**, 259; (b)T. Ikeda, S. Kayamori and F. Mizukami, *J. Mater. Chem.*, 2009, **19**, 5518.
6 M.E. Leonowicz, J.A. Lawton, S.L. Lawton, M.K.Rubin, *Science*, **264**, 1910.
7 (a)A. J. Blake, K. R. Franklin, B. M. Lowe, *J. Chem. Soc., Dalton Trans.*, 1988, 2513; (b)B. Marler, M. A. Camblor, H. Gies, *Microporous Mesoporous Mater.*, 2006, **90**, 87.
8 (a)T. Ikeda, Y. Akiyama, Y. Oumi, A. Kawai and F. Mizukami, *Angew. Chem. Int. Ed.*, 2004, **43**, 4892; (b)D. L. Dorse, and G. J. Kennedy, *J. Phys. Chem. B*, 2004, **108**, 15216; (c) B. Marler, Y. Wang, J. Song and H. Gies, *Dalton Trans.*, 2014, **43**, 10396
9 S. Zanardi, A. Alberti, G. Cruciani, A. Corma, V. Fornes and M. Brunelli, *Angew. Chem. Int. Ed.*, 2004, **43**, 4933.
10 (a) Y. X. Wang, H. Gies, B. Marler, and U. Müller,*Chem. Mater.*, 2005, **17**, 43; (b) Y. X. Wang, H. Gies, and J. H. Lin, *Chem. Mater.*, 2007, **19**, 4181.
11 (a) B. Marler, N. Ströter, H. Gies, *Microporous Mesoporous Mater.*, 2005, **83**, 201; (b) Y. Asakura, S. Osada, N. Hosaka, T.Terasawa and K. Kuroda, *Dalton Trans.*, 2014, **43**, 10392.
12 T. Moteki, W. Chaikittisilp, A. Shimojima and T. Okubo, *J. Amer. Chem. Soc.*, 2008, **130**, 15780.
13 A. Rojas and M. A. Camblor,*Chem. Mater.* 2014, 26, 1161
14 (a) W.J. Roth, P. Nachtigall, R. E. Morris, P. S. Wheatley, V. R. Seymour, S. E. Ashbrook, P. Chlubná, L. Grajciar, M. Položij, A. Zukal, O. Shvets, J. Čejka, *Nat. Chem.*, 2013, **5**, 628; (b) E. Verheyen, L. Joos, K. V. Havenbergh, E. Breynaert, N. Kasian, E. Gobechiya, K. Houthoofd, C. Martineau, M. Hinterstein, F. Taulelle, V. V. Speybroeck, M. Waroquier, S. Bals, G. V. Tendeloo, C. E. A. Kirschock, J. A. Martens, *Nat. Mater.*, 2012, **11**, 1059.
15 A. Burton, R. J. Accardi, R. F. Lobo, M. Falconi, M. W. Deem, *Chem. Mater.*, 2000, **12**, 2936.
16 T. Ikeda, Y. Oumi, K. Honda, T. Sano, K. Momma, F. Izumi, *Inorg. Chem.*, 2011, **50**, 2294.
17 R. Millini, L. C. Carluccio, A. Carati, G. Bellussi, C. Perego, G. Cruciani and S. Zanardi, *Microporous Mesoporous Mater.*, 2004, **74**, 59.
18 L. Massueger, C. Baerlocher, L. B. McCusker and M. A. Zwijnenburg, *Microporous Mesoporous Mater.*, 2007, **105**, 75.
19 D. H. Brouwer, S. Cadars, J. Eckert, Z. Liu, O. Terasaki, B. F. Chmelka, *J. Am. Chem. Soc.*, 2013, **135**, 5641.
20 (a) W. Wan, J. L. Sun, J. Su, S. Hovmöller, X. D. Zou, *J. Appl. Crystallogr.*, 2013, **46**, 1863; (b) P. Guo, L. Liu, Y. Yun, J. Su, W. Wan, H. Gies, H. Zhang, F. Xiao and X. Zou, *Dalton Trans.*, 2014, **43**, 10593
21 R. A. Young, *The Rietveld Method*, Oxford University Press, Oxford, 1993.
22 X. Xue, M. Kanzaki, *J. Phys. Chem. B*, 2007, **111**, 13156.
23 S. Vortmann, J. Rius, S. Siegmann and H. Gies, *J. Phys. Chem. B*, 1997, **101**, 1292.
24 (a) B. Marler, Z. Li, G. Wang, H. Gies, *Acta Cryst.* 2011 A**67,** C650; (b) N. Tsunoji, T. Ikeda, Y. Ide, M. Sadakane and T. Sano, *J. Mater. Chem.*, 2012, **22**, 13682, (c) N. Tsunoji, T. Ikeda, M. Sadakanea and T. Sano, *J. Mater. Chem. A*, 2014, **2**, 3372.
25 A. LeBail, *Powder Diffr.*, 2004, **19**, 249.
26 (a) T. Ikeda, Y. Akiyama, F. Izumi, Y. Kiyozumi, F. Mizukami and T. Kodaira, *Chem. Mater.*, 2001, **13**, 1286; (b) Y. Asakura, R. Takayama, T. Shibue and K. Kuroda, *Chem. Eur. J.*, 2014, **20**, 1893
27 B. Marler, A. Grünewald-Lüke, S. Grabowski, H. Gies, *Z. Kristallogr.*, 2012, **227**, 4247.
28 U. Oberhagemann, P. Bayat, B. Marler, H. Gies and J. Rius, *Angew. Chem. Int. Ed. Engl.*, 1996, **35**, 2869.
29 Z. F. Li, B. Marler and H. Gies, *Chem. Mater.*, 2008, 20, 1896.
30 Y. Oumi, T. Takeoka, T. Ikeda, T. Yokoyama, T. Sano, *New J. Chem.*, 2007, **31**, 593; T. Ikeda, Y. Oumi, T. Takeoka, T. Yokoyama, T. Sano and T. Hanaoka, *Microporous Mesoporous Mater.*, 2008, **110**, 488.
31 (a) G. Jones, in: A. C. Cope (Ed.), Oranic Reactions, vol. 15, John Wiley and Sons, New York, 1967, p. 204; (b) J. March, in: Advanced Organic Chemistry, third ed., John Wiley and Sons, New York, 1985.
32 H. Hattori, *Appl. Catal.*, 2001, **A222**, 247.
33 (a) K. Komura, T. Kawamura, Y. Sugi, *Catal. Commun.*, 2007, **8**, 644; (b) N. Tsunoji, M. Fukuda, K. Yoshida, Y. Sasaki, T. Ikeda, Y. Ide, M. Sadakanea and T. Sano, *J. Mater. Chem. A*, 2013, **1**, 9680

Syntheses, structure solutions, and catalytic performance of two novel layered silicates

Jie Liang,[a] Jie Su,[*b] Yanping Chen,[a] Zhaofei Li,[c] Kuo Li,[a] Hao Zhang,[a] Xiaodong Zou,[b] Fuhui Liao,[a] Yingxia Wang,[*a] and Jianhua Lin[*a]

Table of contents

PKU-13 and PKU-13a, constructed by the same r52 layers by the insertion of mono- and double- layers of SDA molecules respectively, exemplify a structural transformation by the treatment of acetic acid.